JOURNAL OF VIROLOGY, Oct. 2007, p. 10758–10768 Vol. 81, No. 19
0022-538X/07/$08.00+0 doi:10.1128/JVI.00725-07

Role of Endocytosis and Low pH in Murine Hepatitis Virus Strain A59 Cell Entry▽

Patricia Eifart,[1] Kai Ludwig,[2] Christoph Böttcher,[2] Cornelis A. M. de Haan,[3] Peter J. M. Rottier,[3] Thomas Korte,[1]* and Andreas Herrmann[1]*

Humboldt-Universität zu Berlin, Institut für Biologie/Biophysik, Mathematisch-Naturwissenschaftliche Fakultät I, Berlin, Germany[1]; Forschungszentrum für Elektronenmikroskopie, Freie Universität Berlin, Berlin, Germany[2]; and Utrecht University, Faculty of Veterinary Medicine, Department of Infectious Diseases and Immunology, Utrecht, The Netherlands[3]

Received 4 April 2007/Accepted 29 June 2007

Infection by the coronavirus mouse hepatitis virus strain A59 (MHV-A59) requires the release of the viral genome by fusion with the respective target membrane of the host cell. Fusion is mediated by the viral S protein. Here, the entry pathway of MHV-A59 into murine fibroblast cells was studied by independent approaches. Infection of cells assessed by plaque reduction assay was strongly inhibited by lysosomotropic compounds and substances that interfere with clathrin-dependent endocytosis, suggesting that MHV-A59 is taken up via endocytosis and delivered to acidic endosomal compartments. Infection was only slightly reduced in the presence of substances inhibiting proteases of endosomal compartments, precluding that the endocytic uptake is required to activate the fusion potential of the S protein by its cleavage. Fluorescence confocal microscopy of labeled MHV-A59 confirmed that virus is taken up via endocytosis. Bright labeling of intracellular compartments suggests their fusion with the viral envelope. No fusion with the plasma membrane was observed at neutral pH conditions. However, when virus was bound to cells and the pH was lowered to 5.0, we observed a strong labeling of the plasma membrane. Electron microscopy revealed low pH triggered conformational alterations of the S ectodomain. Very likely, these alterations are irreversible because low-pH treatment of viruses in the absence of target membranes caused an irreversible loss of the fusion activity. The results imply that endocytosis plays a major role in MHV-A59 infection and the acidic pH of the endosomal compartment triggers a conformational change of the S protein mediating fusion.

There are two major routes for enveloped viruses to enter a host cell: the endosomal and the nonendosomal pathways (44, 55). In both cases the release of the viral genome requires fusion of the viral envelope with the respective target membrane of the host cell, i.e., the endosomal or the plasma membrane (34).

Fusion is mediated by a conformational change of virus spike-like glycoproteins. For viruses that use the nonendosomal pathway, such as retroviruses (e.g., human immunodeficiency virus type 1) and paramyxoviruses (e.g., Sendai virus) (7, 56), the conformational change of the spike glycoproteins is induced by its interaction with the corresponding receptor on the host cell surface, thereby triggering fusion between the viral envelope and the plasma membrane (4). Other viruses such as orthomyxoviruses (e.g., influenza virus) are taken up by cells via the endosomal pathway. In that case, acidification of late endosomal lumen by proton pump activity of V-type ATPases (45) initiates the conformational change of viral proteins toward the fusion-competent state. Recently, it has been shown for avian sarcoma/leucosis virus that the conformational change of fusion mediating protein requires both receptor priming and low pH (15, 38). There are also examples for viruses utilizing both pathways, e.g., the Japanese encephalitis virus (genus *Flaviviridae*). This virus is able to enter the cells either through fusion at the plasma membrane or upon uptake through endocytosis (41).

The mouse hepatitis virus (MHV) belongs to the coronavirus family. It causes enteric and respiratory infection, diarrhea, hepatitis, and acute or chronic demyelination of the central nervous system (52, 65). As typical for coronaviruses, binding of MHV and fusion with the target membrane of the host cells is mediated by the spike glycoprotein (S). The S protein, a class I viral glycoprotein (6), is organized as a homotrimer with a molecular mass of approximately 180 kDa per monomer. During maturation of the virus, the MHV S protein is cleaved by cellular proteases into two subunits (12, 16): a receptor-binding S1 subunit and a fusion-mediating S2 subunit. Although previous reports indicate that the cleavage of the S glycoprotein into the S1 and S2 subunit at the cleavage site is not strictly required for fusion of coronaviruses (5, 12, 21), recent studies have shown that cleavage of the ectodomain is essential for fusion and may occur only in the endosomal compartment of cells being infected (8, 48, 54). The S2 domain harbors the transmembrane domain, the fusion peptide, and two heptad repeat (HR) sequences. The latter two sequences, HR1 and HR2, have been shown to form coiled-coil structures in vitro (6, 68, 69). Formation of the coiled-coil motif and exposure of the fusion peptide toward the target membrane are major steps of the fusion-mediating conformational change of class I fusion proteins (for a review, see reference 15).

MHV-A59, a substrain of MHV, binds to the CEACAM1a receptor on murine cells via the S protein. Entry of MHV appears to be strongly raft-associated and thus cholesterol

* Corresponding authors. Mailing address: Institut für Biologie/Biophysik, Humboldt-Universität zu Berlin, Invalidenstr. 42, D-10115 Berlin, Germany. Fax: 49 30 2093 8585. E-mail for T. Korte: thomas.korte@rz.hu-berlin.de. E-mail for A. Herrmann: andreas.herrmann@rz.hu-berlin.de.

▽ Published ahead of print on 11 July 2007.

dependent (9, 61). Although cholesterol depletion of the plasma membrane does not affect virus attachment, MHV-A59 infection is efficiently inhibited (9, 61). However, it is not known which of the two major pathways of viral entry, the endosomal or nonendosomal, MHV-A59 accomplishes. For MHV, indications for both pathways have been reported (29, 37, 39). Holmes et al. (25) observed fusion of the MHV with the target cell through receptor binding, which was suggested to initiate a conformational change toward the fusion-competent state. Recent studies revealed a major role for the N-terminal part of the CEACAM1a receptor to induce a conformational change in the spike glycoprotein (35, 36, 73). Earlier studies observed that after MHV-A59 infection cell-cell fusion takes place at a neutral pH mediated by the spike glycoprotein expressed partially at the plasma membrane (16). However, other studies show a clear attenuation of MHV infection after treatment of the host cells with lysosomotropic agents (12, 31, 37), which are known to prevent acidification of the endosomal compartment, implying that the endosomal pathway may be utilized by MHV. For example, infectivity was delayed for MHV-A59-infected L2 cells treated with ammonium chloride (37). Krzystyniak and Dupuy (31) reported that infection by MHV-3 is sensitive to lysosomotropic agents. Although it was initially suggested that wild-type MHV-4 (JHM) enters cells in culture by a pH-independent pathway (17), later studies show that MHV-JHM utilizes either the endosomal or the nonendosomal pathway depending on the cell type (39).

In the present study we investigated the infection of mouse fibroblast cells by MHV-A59 and studied directly the fusion of the viral envelope with the respective target membranes by using various complementary and independent approaches such as plaque titration assay, fluorescence microscopy, spectroscopy, and electron microscopy. Our data provide evidence that the endocytic pathway is the major route of MHV-A59 cell entry and that infection of host cells by MHV-A59 requires a low-pH trigger. Preincubation of MHV-A59 at acidic pH abolished fusion activity, suggesting that low pH triggers a conformational change of the S protein that is irreversible.

MATERIALS AND METHODS

Cells and viruses. For infection with MHV, 17Cl-1 cells, a spontaneously transformed cell line of BALB/c 3T3 cells, LR-7 (L-cell derivate), and DBT cells, a murine astrocytoma cell line (22), were used. The CEACAM receptor was cloned into LR-7 cells to enhance infectibility by MHV (12). All cell lines were propagated in Dulbecco modified Eagle medium, Invitrogen, Karlsruhe, Germany) supplemented with 10% fetal calf serum (Invitrogen) (DMEM-10% FCS), penicillin (100 U/ml), and streptomycin (100 μg/ml) (Pen/Strep; Biochrom AG, Berlin, Germany). MHV-A59 virions kindly provided by J. Ziebuhr (University of Würzburg) were grown on 17Cl-1 cells and assayed by plaque titration as described previously (59). For control experiments a recombinant MHV expressing the S protein of JHM (MHV-S4) and vesicular stomatitis virus (VSV) strain Indiana were used. MHV-A59 FI, a virus with an uncleaved spike protein, was generated as described previously (12). Viral infection medium was composed of DMEM supplemented with 2% FCS (DMEM-2%) and antibiotics as described above.

Virus production and purification. Monolayers of 17Cl-1 cells (59) were grown in T175 flasks and inoculated with MHV-A59 or MHV-S4 at a multiplicity of 10 PFU per cell (PFU/cell). For generation of MHV-A59 with uncleaved spike proteins (MHV-A59 FI), cells were treated with 75 μM furin inhibitor (FI) peptidyl chloromethylketone (dec-RVKR-cmk) (12) and infected with MHV-A59 in the presence of the inhibitor at an MOI of 10 PFU/cell. Cells and viruses were incubated for 1 h at 37°C for attachment of the virus. After the adsorption period, 20 ml of DMEM-2% was added to each flask, followed by incubation for at least 48 h at 37°C and 5% CO_2. Virus was collected 46 to 48 h after inoculation. The supernatant containing released virus was first centrifuged at 10,000 × *g* in a Beckman JA 25.50 rotor for 30 min at 4°C to remove cellular debris.

For precipitation of the virus, 5.0 g of NaCl and a half volume of 30% polyethylene glycol (8 kDa; Promega, Mannheim, Germany) were added to the virus supernatant to achieve a final concentration of 10% polyethylene glycol and 2.2% NaCl, and incubation was carried out for 4 h at 4°C. Centrifugation at 10,000 × *g* for 30 min at 4°C was accomplished in a Beckman JA 25.50 rotor to harvest the precipitated virus. The viral pellet was suspended in BisTris-buffered saline (pH 6.5) at 4°C and purified through a discontinuous gradient of 5 ml each of 30 and 50% (wt/wt) sucrose (Sigma Aldrich, Munich, Germany) in BisTris-saline (pH 6.5) in a 12-ml centrifuge tube. Centrifugation for 16 h in a Beckman SW40 Ti rotor was carried out at 28.000 rpm (110,000 × *g* average) at 4°C. The virus band at the interface between 30 and 50% sucrose was collected, divided into aliquots, and frozen at −80°C. Virus collected 46 to 48 h postinfection (p.i.) had a titer of 1×10^9 to 2×10^9 PFU/ml (for determination, see below). For the experiments, viruses were dialyzed against BisTris-buffered saline (pH 6.5; 150 mM NaCl and 25 mM BisTris) with 5% glycerol.

Plaque assay. Virus titers were determined by plaque titration assay. Cell monolayers were cultured in six-well culture plates (Nunc, Wiesbaden, Germany) and inoculated with serial log dilutions of virus. For adsorption, virions and cells were incubated for 1 h at 37°C. Afterward, the inoculum was removed and replaced by overlay medium (DMEM–2% FCS, 0.75% Oxoid agarose [Oxoid, Hampshire, United Kingdom]). After incubation for at least 20 to 24 h, the plaques were visualized by neutral red staining (33.3% [wt/vol] stock solution; Sigma-Aldrich, Munich, Germany).

Plaque reduction assay. To measure the inhibitory effect of lysosomotropic agents on virus production, cells were treated with either 10 μM monensin, 100 nM bafilomycin A1, 10 nM concanamycin A, or 20 mM ammonium chloride (NH_4Cl). To assess whether intracellular proteases may affect virus infection, cells were pretreated with the protease inhibitors E-64 (10 μM) and leupeptin (10 μg/ml). To inhibit endocytosis, cells were pretreated with chlorpromazine (15 μM). Monensin, bafilomycin A1, and concanamycin A were prepared in ethanol. Ammonium chloride and chlorpromazine-HCl were solubilized in water. The protease inhibitors were prepared in dimethyl sulfoxide (DMSO). Ethanol and DMSO concentrations during the experiments remained below 1 vol%. Cells were pretreated with substances for 30 min at 37°C before virus infection. All drugs used were present throughout the infection period. To assess the role of cholesterol for MHV-A59 infection, cells were depleted of cholesterol by incubation with 15 mM methyl-β-cyclodextrin (MβCD) for 30 min at 37°C. Subsequently, cells were washed twice with phosphate-buffered saline (PBS). In another set of experiments the cells were incubated with 5 μg of Filipin III/ml for 30 min at 37°C. Filipin is known to form complexes with cholesterol (9). To assess the viability of cells upon treatment with various compounds, the cells were stained with DAPI (4′,6′-diamidino-2-phenylindole). DAPI is known to enter nonviable cells and to stain the cell nuclei. Staining was monitored by fluorescence microscopy.

After treatment, cells were infected with the respective virus at a multiplicity of 1 PFU/cell or incubated with log dilutions. Virus titers were quantified by plaque titration or plaque assay at 20 to 24 h postinoculation. As a control the cells were treated with corresponding amounts of the solvents (ethanol or DMSO), and virus titers were determined by plaque assay. For some experiments cells were treated with the lysosomotropic agents ammonium chloride (20 mM) or bafilomycin A1 (100 nM), and virus was subsequently bound to the cells. Virus-cell complexes were treated with acidic buffer to lower the pH of the medium to 5.0 for 5 min at 37°C. Upon neutralization, a plaque titration assay was carried out as described before.

Labeling of virus. Labeling of MHV-A59 with octadecylrhodamine-B-chloride (R_{18}; Molecular Probes, Munich, Germany) at a self-quenching concentration (23) was done by incubating 100 μl of 2 mg of MHV-A59/ml in BisTris-sucrose buffer (pH 6.5), with 0.5 μl of 2.2 mM R_{18} in ethanol for 30 min at 700 rpm shaking in the dark as described previously for influenza virus A (30) and respiratory syncytial virus (43). Unbound dye was removed by centrifugation at 55,000 × *g* for 10 min at 4°C. The virus was suspended in 100 μl of ice-cold PBS. As verified by fluorescence spectroscopy (see below), nearly 90% of the fluorescence was quenched in the viral membrane. Labeling of the virus did not affect infection of cells, as revealed by a plaque titration assay.

Microscopy. Subconfluent 17Cl-1 cells in 35-mm-by-14 mm^2 glass-bottom dishes (MaTek, Ashlands, MA) were incubated with labeled MHV-A59 at a multiplicity of 5 to 10 PFU/cell for 15 min at 4°C for viral attachment. For pretreatment of the cells see above. To remove unbound viruses, cells were washed two times with ice-cold PBS. Afterward, virus-cell complexes were incubated at different pHs ranging from 5.0 to 7.0 for 5 to 30 min at 37°C. As a control, nonpermissive cells were treated in the same manner. Syncytium for-

mation after infection of different mouse cell lines with MHV-A59 or MHV-S4 was analyzed by light microscopy at 24 h p.i. All samples were immediately analyzed by fluorescence microscopy using an Olympus IX81 microscope equipped with a cooled charge-coupled device camera SPOT RT Slider (Diagnostic Instruments, Sterling Heights, United Kingdom). Image acquisition and analysis was done by using MetaView software (Universal Imaging, Buckinghamshire, United Kingdom). Cell-virus complexes were also analyzed with a FluoView FV-1000 confocal microscope (Olympus, Hamburg, Germany); R_{18}-labeled MHV-A59 viruses were imaged by using 543-nm laser excitation and band pass 590- to 655-nm emission wavelength. An oil-immersion objective lens (Olympus) with ×60 magnification and a numerical aperture of 1.35 was used. All experiments were performed at 37°C and the microscopy was carried out at room temperature. The image processing was done by using the MetaMorph-Software (Universal Imaging), and further processing was carried out by using Adobe Photoshop 7.0 and Adobe Illustrator 10.0 (Adobe Systems GmbH, Munich, Germany). For the editing of confocal images, Olympus FluoView software (version 1.4a; Olympus) was used.

Spectroscopic fluorescence dequenching assay. For the fluorescence dequenching assay, 17Cl-1 cells were grown in T75 flasks and harvested by treatment with trypsin. Labeled virions were suspended in ice-cold PBS and allowed to bind to 17Cl-1 cells at a multiplicity of 3 to 5 PFU/cell for at least 40 min on ice in the dark with gentle mixing. To remove unbound viruses, the virus-cell suspension was centrifuged at 300 × *g* for 5 min and washed twice with ice-cold PBS. Fusion of labeled MHV-A59 with 17Cl-1 cells was measured by the R_{18} dequenching assay at 4 and 37°C (23). This fusion assay is based on the redistribution of R_{18} from the viral envelope to the target membrane of the cell after fusion, leading to a dequenching and thus an increase of the fluorescence emission of R_{18}. Fusion was monitored over time by using a spectrofluorimeter (AMINCO-Bowman, Urbana, IL) with an excitation wavelength of 560 nm and an emission wavelength of 590 nm (cutoff filter, 570 nm; time resolution, 1 s). I_0 is the fluorescence intensity of the labeled virus bound to target cells at time point $t = 0$. Thereafter, the time-dependent fluorescence intensity $I(t)$ was recorded for at least 30 min at various pH. Subsequently, to determine the maximum of fluorescence dequenching (100%), 0.2% Triton X-100 was added to the cuvette, and the maximum intensity (I_{max}) was measured. The extent of fusion (F) is proportional to percent fluorescence dequenching maximum and is defined as (3):

$$F = \frac{I(t) - I_0}{I_{max} - I_0} \times 100\%$$

In some cases, viruses were pretreated in acidic buffer (pH 5.0) for 15 min at 37°C and subsequent to neutralization bound to cells, and fusion was measured by dequenching of the R_{18} at 37°C as described above.

Cryoelectron microscopy. Preincubated sample droplets were applied to perforated (1-μm hole diameter) carbon film-covered 200 mesh grids (R1/4 batch of Quantifoil [MicroTools GmbH, Jena, Germany]), which had been hydrophilized before use by 60-s plasma treatment at 8 W in a BALTEC MED 020 device. The supernatant fluid was removed with a filter paper until an ultrathin layer of the sample solution was obtained spanning the holes of the carbon film. The samples were immediately vitrified by propelling the grids into liquid ethane at its freezing point (90 K) with a guillotine-like plunging device. The vitrified samples were subsequently transferred under liquid nitrogen into a Philips CM12 transmission electron microscope (FEI, Oregon) using a Gatan (Gatan, Inc., California) cryoholder and stage (model 626). Microscopy was carried out at a 94 K sample temperature using the low-dose protocol of the microscope at a primary magnification of ×58,300 and an accelerating voltage of 100 kV (LaB6-illumination). The defocus was set to 1.5 μm.

"Negative-stain" electron microscopy. Preincubated sample solution was absorbed onto hydrophilized carbon film that covered the copper grids (400 mesh). The supernatant fluid was removed by blotting with a filter paper, and the sample was allowed to dry in air. Contrast-enhancing heavy-metal stain solution (1% phosphotungstic acid at pH 7.4) was subsequently applied for 45 s and blotted again. A standard holder was used to transfer the dried samples into a Philips CM12 transmission electron microscope (FEI) equipped with a LaB_6 cathode. Images were taken at a defocus value of 0.6 μm using a primary magnification of ×58,300 at an accelerating voltage of 100 kV (C_s = 2 mm).

RESULTS

Infection by MHV-A59 is sensitive to lysosomotropic agents and inhibitors of endocytosis. To explore whether MHV-A59 cell entry proceeds via the endocytic uptake and infection requires the acidic environment of late endosomes, we inhibited this pathway by using substances either interfering with endocytosis and/or with endosomal acidification (33). To the former belong chlorpromazine, which is known to inhibit the formation of clathrin-coated vesicles (64) and thus clathrin-dependent endocytosis (2, 13, 53, 60). To prevent endosomal acidification, we used such lysosomotropic agents as (i) ammonium chloride, a relatively weak base accumulating inside endosomal vesicles (18, 24, 37, 48); (ii) monensin, an ionophore that disrupts the proton gradient across vesicular membranes (39, 40, 42, 45); and (iii) bafilomycin A1 and concanamycin A, specific inhibitors of the vacuolar H^+-ATPase (V-ATPase) in animal and other eukaryotic cells (14, 18, 27, 45). Concentrations of substances were chosen according to previous studies showing the inhibition of infection of other enveloped viruses entering the cell via the endocytic route (1, 2, 13, 20, 28, 31, 37, 45, 60, 62, 72). Treatment with these agents did not interfere with cell viability since staining of cells with DAPI was not enhanced with respect to control cells (data not shown).

To assess the infection of 17Cl-1 cells by MHV-A59 and the influence of the above substances, we used the plaque assay (see Materials and Methods). All lysosomotropic agents used showed a strong inhibitory effect on virus infection (Fig. 1A). At concentrations of 20 mM ammonium chloride a plaque reduction of more than 50% was observed. The inhibitory effect of the other lysosomotropic substances was even more striking. Virus replication was almost completely abolished at concentrations as low as 10 nM for concanamycin A, 100 nM for bafilomycin A1, and 10 μM for monensin (Fig. 1A). Attenuation of virus infection was also observed upon treatment of cells by inhibitors of endocytosis. At a concentration of 15 μM chlorpromazine, infection was inhibited completely (Fig. 1A). Taken together, these results strongly argue for a clathrin-dependent endocytic uptake as the main cell entry route for MHV-A59 and for a low-pH environment in the endosome as presuppositions to release the viral genome into the cytoplasm.

Similar experiments were carried out with LR-7 and DBT cells, different mouse cell lines previously described to be infected by MHV-A59. Infection of these cell lines showed the same response to incubation with lysosomotropic agents and agents interfering with the clathrin-dependent entry pathway such as ammonium chloride, bafilomycin A1, monensin, and chlorpromazine as observed for 17Cl-1 cells. Infectivity was completely blocked after incubation with either 100 nM bafilomycin A1, 10 μM monensin, or 15 μM chlorpromazine (Fig. 1A). In the case of ammonium chloride infectivity could be reduced up to 70 or 100% (Fig. 1A). These results are in agreement with the previously observed delay in MHV-A59-infected L2 cells after treatment with ammonium chloride (37). In contrast to MHV-A59, the recombinant virus MHV-S4 expressing the S-protein of JHM and known to enter the host cell via the clathrin-independent, nonendocytic pathway (29, 31) preserved its infectivity after treatment of the cells (17Cl-1, LR-7, or DBT) with ammonium chloride or bafilomycin A1 (Fig. 1B). For LR-7 and DBT cells, both ammonium chloride and bafilomycin A1 had only a minor effect on cell infection compared to the control (absence of lysosomotropic agents) (Fig. 1B, gray bars). For MHV-S4-infected 17Cl-1 cells we also did not find any block of infectivity after incubation with am-

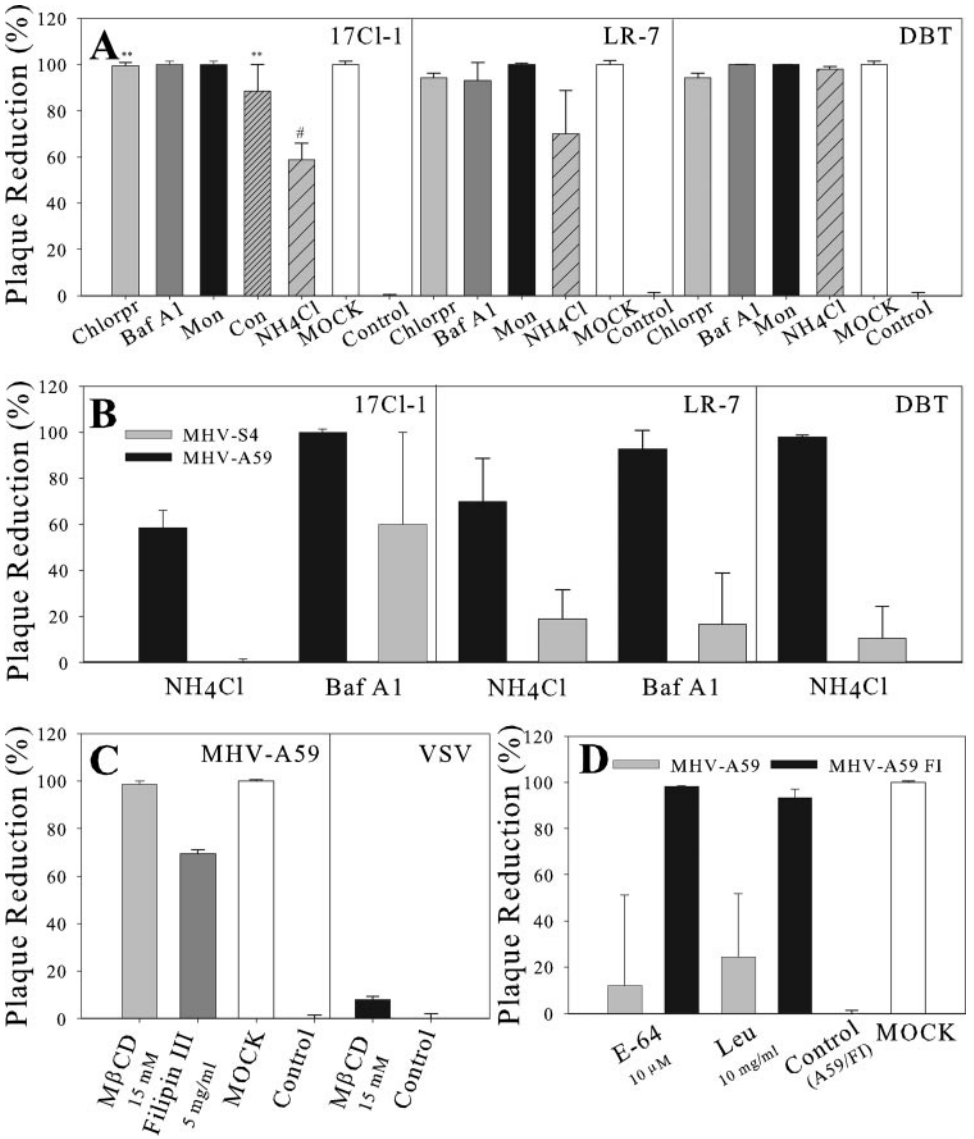

FIG. 1. Inhibition of MHV-A59 infection of different murine cells by substances interfering with the endocytic pathway and endosomal acidification. Infection by MHV-A59 was assessed by plaque assay. (A) Infection of 17Cl-1, LR-7, and DBT cells by MHV-A59 in the presence of chlorpromazine-HCl (Chlorpr; 15 μM, gray bar), bafilomycin A1 (Baf A1; 100 nM, dark gray bar), monensin (Mon; 10 μM, black bar), concanamycin A (Con; 10 nM, striped gray bar), and ammonium chloride (NH_4Cl; 20 mM, gray hatched bar). (B) Cells were treated with 20 mM ammonium chloride (NH_4Cl) or 100 nM bafilomycin A1 (Baf A1) and infected with either MHV-A59 (black bar) or MHV-S4 (gray bar) in the presence of the drug. (C) Influence of cholesterol depletion of 17Cl-1 cells on infection by MHV-A59. Bars: light gray, cholesterol depletion by MβCD treatment; dark gray, preincubation of cells with Filipin III. For treatment of the cells with substances, see Materials and Methods. As a control, VSV, which is known to enter cells independently of cholesterol and/or rafts, was used (black bar). (D) Influence of the protease inhibitors E-64 and leupeptin on infection of 17Cl-1 cells with MHV-A59 (gray bar) and MHV-A59 FI (black bars). The data present means ± the standard errors of estimates of three independent experiments unless otherwise indicated (**, $n = 2$; #, $n = 5$).

monium chloride (Fig. 1B). Infectivity was also preserved in the presence of bafilomycin A1. However, in that case infectivity was not completely restored but only to ca. 40% (Fig. 1B, left, gray bar).

We also probed for syncytium formation of 17Cl-1 cells after infection with viruses and did not observe any syncytia for MHV-A59-infected cells at 24 h postinoculation. By 48 h p.i. only a minority of cells had undergone syncytium formation. In contrast, significant syncytium formation was found for MHV-S4 at 24 h p.i. (data not shown). These results show that the infection pathway of MHV-S4 (JHM) does not require an acidic environment as observed for MHV-A59. The partial inhibition of infection of 17Cl-1 cells by bafilomycin A1 which was not observed for LR-7 cells is in agreement with previous observations of Nash and Buchmeier (39) showing that MHV-JHM may utilize different cell entry pathways depending on the cell type. Furthermore, these results provide evidence that the viability of cells is not affected by treatment with lysosomotropic substances and agents interfering with the clathrin-dependent pathway.

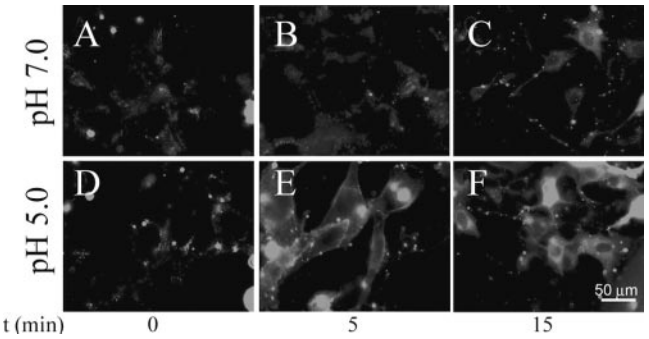

FIG. 2. Low pH triggers fusion of MHV-A59 with the plasma membrane of 17Cl-1 cells. R_{18}-labeled virus was bound to cells. Subsequently, virus-cell complexes were incubated at 37°C under neutral (pH 7.0, A to C) or acidic (pH 5.0, D to F) conditions and observed by fluorescence microscopy. (E) Mild acidic conditions (pH 5.0) mimic the acidic pH of endosomal compartments and enable the virus to directly fuse at the plasma membrane, as indicated by strong labeling of the plasma membrane already after 5 min of incubation at 37°C. No significant fusion of viruses with the plasma membrane was observed at pH 7.0 (panels A to C). After 15 min (see panel C), some intracellular staining was observed. For further explanations, see Results. Bar, 50 μm.

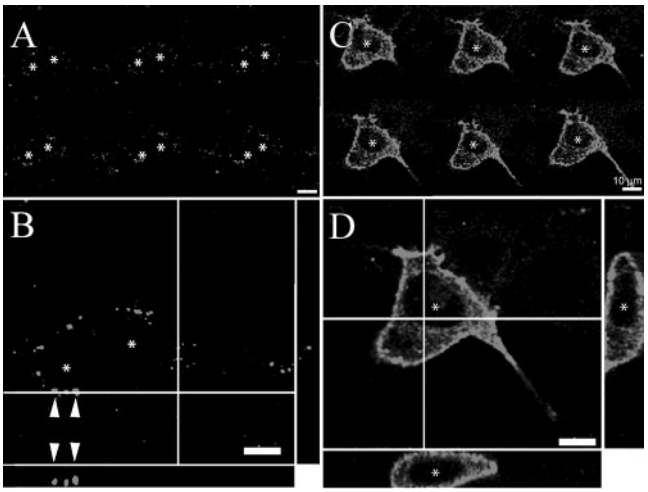

FIG. 3. Interaction of MHV-A59 with 17Cl-1 cells studied by confocal fluorescence microscopy. R_{18}-labeled virus was bound to cells. Subsequently, virus-cell complexes were incubated at 37°C under neutral (pH 7.0, A and B) or at acidic conditions (pH 5.0, C and D) for 30 or 5 min, respectively, and imaged by confocal fluorescence microscopy. To characterize the labeling pattern a three-dimensional stack analysis was performed. In panels A and C selected z-planes are shown, while in panels B and D a plot of fluorescence along the *x* and *y* coordinates provide respective side views of the cells. At neutral pH the viruses are delivered to intracellular compartments (B, arrowheads) (for further details, see Results and Discussion). When virus-cell complexes were incubated at low pH, a strong labeling of the plasma membrane was observed (D) that was not seen for incubation at neutral pH. Bars, 10 μm. Asterisks mark the positions of the nuclei.

Recent studies provided evidence that cell entry of enveloped viruses is associated with lipid domains harboring cholesterol (9, 10, 50, 61). After cholesterol depletion of 17Cl-1 cells by preincubation with 15 mM MβCD (see Materials and Methods), virus infection was completely blocked (Fig. 1C). A 70% reduction of virus infection was found when cells were pretreated with 5 μg of filipin/ml; filipin is known to form complexes with cholesterol (Fig. 1C). These findings confirm the importance of cholesterol for MHV-A59 infection (9, 61). As a control, 17Cl-1 cells were infected with VSV, which is known to enter cells independently of cholesterol and/or rafts (19, 46). Only a minor reduction of infectivity of ca. 8% occurred after cholesterol depletion of the cells by MβCD (Fig. 1C, black bar).

Protease inhibitors do not interfere with infection by MHV-A59. There is now strong evidence that cleavage of the S protein of coronaviruses is an essential determinant of fusion activity. Depending on the virus strain, cleavage may occur already during virus maturation in the host cell. However, recently it has been shown that the cleavage of the S proteins of coronaviruses such as SARS and MHV-2 is mediated only by endosomal proteases of the infected cells (8, 26, 48, 54). To address whether the activity of those proteases may play a role in infection by MHV-A59, we studied infection of 17Cl-1 cells in the presence of leupeptin and E-64, which have been shown to inhibit acidic proteases in the endosomal compartment. These inhibitors were tested at appropriate concentrations formerly used (8, 48, 54). We observed only a minor effect of the inhibitors on virus infectivity (Fig. 1D, gray bars). Viral replication was only reduced by ca. 20% for leupeptin (10 μg/ml) or 30% in the case of E-64 (10 μM), respectively. Hence, endosomal protease activity does not seem to play a major role in infection by MHV-A59. To confirm that the used concentrations of protease inhibitors are effective, 17Cl-1 cells were infected with MHV-A59 FI expressing uncleaved spike protein (see Materials and Methods). While in the absence of protease inhibitors infection was similar to that of MHV-A59 (control), infection with MHV-A59 FI was strongly inhibited in the presence of the protease inhibitors leupeptin and E-64 (Fig. 1D, black bars).

Fusion of MHV-A59 monitored by fluorescence microscopy. For visualization of MHV-A59 fusion, virions were labeled with the lipid-like fluorophore R_{18}. Notably, R_{18} labeling of MHV-A59 had no effect on viral infectivity as tested by plaque titration assay (data not shown). Labeled virus was bound to 17Cl-1 cells on ice. Subsequently, virus-cell complexes were incubated at 37°C at neutral pH (pH 7.0) or at pH 5.0 to mimic the endosomal acidic pH. At time $t = 0$ of the incubation, we observed only punctate fluorescence corresponding to viruses attached to the plasma membrane. According to the size of the fluorescence spots, a significant number of viruses may be colocalized or aggregated (Fig. 2). Although a similar fluorescence pattern was found when virus cell-complexes were incubated for 5 min at pH 7.0, we observed R_{18} labeling of the intracellular compartments after incubation of virus-cell complexes for 15 min at pH 7.0 at 37°C (Fig. 2C). We surmise that the latter labeling pattern reflects the localization of MHV-A59 in the endosome and perhaps fusion with endosomal membranes (see below). This is supported by the observation that no intracellular labeling was observed after incubation for 15 min at pH 7.0 at room temperature (data not shown). It is known that at such temperatures endocytosis is strongly diminished (63).

In contrast to the incubation at pH 7.0, we observed a bright spreading of the dye over the plasma membranes already after 5 min of incubation at pH 5.0 and 37°C, indicating efficient

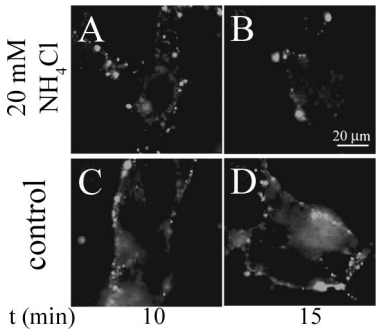

FIG. 4. Incubation of virus-cell complexes with ammonium chloride prevents intracellular staining at pH 7.0. 17Cl-1 cells were either pretreated (A and B, 20 mM ammonium chloride) or not treated (C and D, control) at 37°C for 30 min (see Materials and Methods). Subsequently, R_{18}-labeled viruses were bound to the cells, and virus-cell complexes were incubated at 37°C for the indicated time. For cells pretreated with ammonium chloride (A and B), only a faint intracellular fluorescence was observed, while in untreated cells (C and D) significantly brighter fluorescence labeling was detected. Bar, 20 μm.

fusion of the viral envelope with the plasma membrane (Fig. 2E). Further incubation (t = 15 min) did not enhance labeling of the plasma membranes (Fig. 2F).

To confirm and to characterize the pH-dependent labeling pattern of virus-cell complexes in detail, we performed confocal microscopy. When 17Cl-1 cells were incubated with R_{18}-labeled MHV-A59 for 30 min at 37°C at neutral pH, we found fluorescently labeled cellular organelles that presumably correspond to endosomes loaded or fused with viruses (Fig. 3A and B, arrowheads), as revealed by a z-stack of confocal images (Fig. 3A) and confirmed by a plot of fluorescence along the x and y coordinates, providing respective side views of the cell (Fig. 3B). No spreading of label in the plasma membrane was observed. Occasionally, we found punctate fluorescence sites at the plasma membrane of control cells even after 30 min.

On the contrary, when virus cell complexes were incubated for 5 min at pH 5.0 and 37°C a bright continuous fluorescence over the entire plasma membrane was observed (Fig. 3C and D), confirming the fusion of viruses with the plasma membrane.

To clarify whether the intense punctate intracellular R_{18} fluorescence at neutral pH is associated with fusion of the viruses with endosomal membranes, we preincubated 17Cl-1 cells with 20 mM ammonium chloride and studied the intracellular labeling pattern after incubation of virus-cell complexes at pH 7.0 and 37°C for 30 min (Fig. 4). For control cells not treated with ammonium chloride (Fig. 4C and D), an intracellular staining similar to that already described above was detected (see Fig. 2). However, for cells preincubated with ammonium chloride the intracellular fluorescence was significantly diminished and rather weak (Fig. 4A and B). We surmise that although viruses have been internalized, fusion is inhibited by the lysosomotropic activity of ammonium chloride in the endosomal compartments. Results similar to those for ammonium chloride were obtained for cells treated with bafilomycin A1 (data not shown).

Fusion of MHV-A59 monitored by fluorescence spectroscopy. To confirm our microscopic observation that low pH efficiently triggers the fusion of viruses with the plasma membrane, we studied virus-cell fusion in a cuvette experiment by using a fluorescence dequenching lipid mixing assay (see Materials and Methods) (23). Viruses labeled with R_{18} at self-quenching concentrations were bound to the cells. Subsequently virus-cell complexes were incubated in a cuvette at neutral pH and 37°C for 200 s; afterward, the pH of the suspension medium was lowered to pH 5.0. We observed a strong and rapid increase of the fluorescence intensity, which can be ascribed to a relief of self-quenching upon fusion of the viral envelope with the plasma membrane of 17Cl-1 cells (Fig. 5A). After 600 s at low pH, ca. 25 to 30% of viruses have been fused. Longer incubation caused a further moderate fluorescence dequenching, which leveled off by ca. 40% of fused viruses. Dequenching was temperature dependent. At room temperature we still observed a significant dequenching but to a much lower extent (Fig. 5B). In contrast, at neutral pH we observed a small increase in the fluorescence intensity at 37°C (Fig. 5A), much lower than that observed at pH 5.0. We surmise that this slow

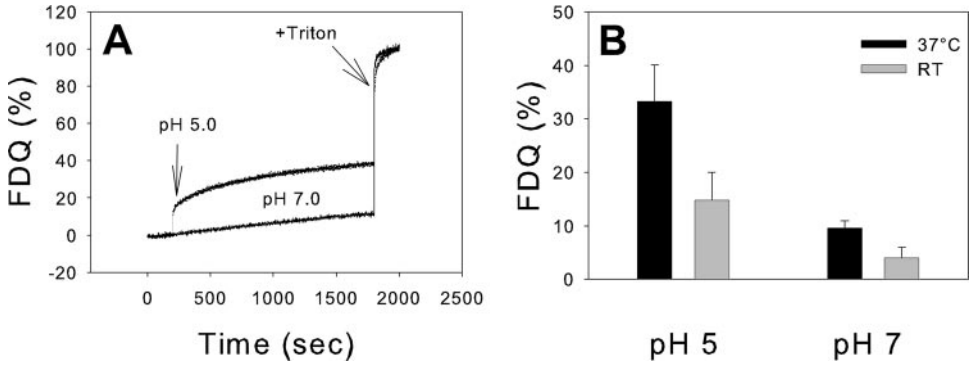

FIG. 5. Fusion of MHV-A59 with 17Cl-1 target cells is triggered by low pH. After binding of R_{18}-labeled viruses to 17Cl-1 cells, virus-cell complexes were suspended, and fluorescence dequenching was measured (see Materials and Methods). (A) Time course of R_{18} fluorescence dequenching measured at neutral and acidic pH and 37°C. The pH was lowered by the addition of appropriate amounts of citric acid (arrow). At the end of the experiment Triton X-100 (arrow) was added to achieve complete fluorescence dequenching. (B) Extent of fusion after measuring fluorescence dequenching for 30 min at 37°C (■) and room temperature (▨). The data present the means ± the standard errors of estimates of at least three independent experiments.

dequenching could be due to unspecific dye transfer from bound viruses to the plasma membrane and/or to intracellular fusion of endocytosed viruses. At 4°C no dequenching could be detected under either of the described conditions (data not shown).

These results show that fusion of MHV-A59 with the plasma membrane can be triggered by acidification. In order to address whether this fusion is productive leading to infection and, eventually, to maturation of new viruses, 17Cl-1 cells were treated with lysosomotropic agents to inhibit virus infection (see above). Subsequently, virus was bound to the cells, and the pH of the virus-cell complex suspension was lowered to 5.0 for 5 min at 37°C. After neutralization a plaque assay was performed (see Materials and Methods). We observed only a partial, rather low restoration of infectivity. Whereas infection was almost completely abolished upon treatment of cells with bafilomycin A1 (~100% plaque reduction; see Fig. 1A), incubation of virus-cell complexes at pH 5.0 caused an infection of ca. 15% (~85% plaque reduction; data not shown). A similar enhancement of infectivity was observed for treatment with 20 mM ammonium chloride (data not shown).

Low pH triggers a conformational change of the spike glycoprotein of MHV-A59. From the results presented above we surmise that the S protein of MHV-A59 undergoes a conformational change at acidic pH triggering fusion. To address the question of whether a conformational alteration is triggered under the conditions used, we studied the shape of spike glycoproteins by transmission electron microscopy (TEM).

At neutral pH we observed spherical viruses with well-defined spike proteins, being about 20 nm in length and consisting of a stalk and a head region distal from the envelope (Fig. 6A, negative-stain TEM, and Fig. 6E, cryo-TEM). This structure is consistent with that found by Sturman et al. (57), who described rosettes of the S protein with a similar shape. After incubation of MHV-A59 at pH 5.0, 37°C, some alterations of the S-protein shape were observed (Fig. 6B to D). We found various arrangements of the spike proteins very likely reflecting different intermediates of a conformational change. For some viruses we could still identify spikes (Fig. 6B). In that case, differences in spike morphology were visually not detectable. If present, these differences could be only identified by image processing. For many viruses, spikes could hardly be detected (Fig. 6D), indicating a fuzzy structure of the S protein. Most remarkably, we often could identify elongated and rather thin stems without any head (see Discussion) (Fig. 6C, arrowheads).

Irreversible loss of fusion activity after preincubation at acidic pH. Next, we addressed whether the structural alterations of the S protein at an acidic pH are irreversible. If so, we surmised that fusion activity should become irreversibly lost by preincubation of the virus in the absence of the target membrane. To test this, we studied the fusion activity of MHV-A59 at low pH after preincubation of R_{18}-labeled viruses at pH 5.0 either at 37 or at 4°C. Before binding to the cells, the suspension medium of viruses was readjusted to neutral pH. Subsequently, virus-cell complexes were incubated at pH 5.0 or 7.0 and 37°C and then examined by fluorescence microscopy, as shown previously. The fusion activity of viruses that were preincubated at 37°C was completely abolished (Fig. 7A and C), while efficient fusion was still found for viruses preincubated at 4°C (Fig. 7B and C). Therefore, we conclude that at low pH and elevated temperatures an irreversible conformational change of the S protein is triggered. To address this notion, we performed a plaque assay with nontreated or low-pH-pretreated virus. Infectivity was reduced up to 60% after preincubation of the virus at acidic pH and 37°C (Fig. 7D, plaque assay). A reduction of fusion activity upon low-pH pretreatment could also be monitored by fluorescence dequenching, where the fusion extent dropped from ca. 40% to less than 10% (Fig. 7D).

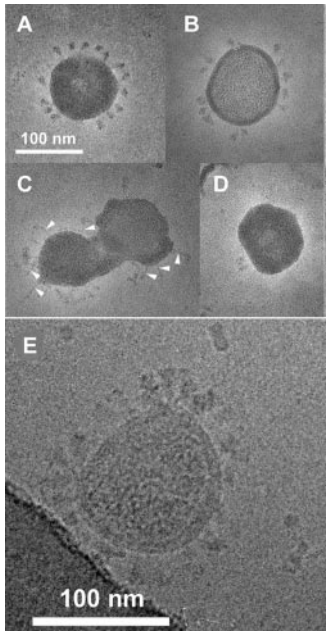

FIG. 6. Low pH triggers a conformational change of the S protein. (A) Negative-stain electron micrograph of MHV-A59 at pH 7.4 and 37°C. Round-shaped virus with several spike proteins on the surface can be seen. The spike proteins consist of a stalk and a distal head domain. (B to D) Negative staining of the electron micrograph of MHV-A59 after incubation of the virus for 5 min at pH 5 and 37°C. The number of visible spike proteins tends to be reduced. We also observed viruses with no visible spikes on the surface (D) and viruses with thin, elongated spike proteins (C). (E) Cryo-electron micrograph of MHV-A59 (without stain) at neutral pH as a control. Bars, 100 nm.

DISCUSSION

To examine the entry pathway of MHV-A59 into murine cells, we used essentially two independent and complementary approaches. First, the plaque assay to assess the infection of cells by viruses. Second, fluorescence microscopy was used to monitor the entry of viruses into cells and the fusion of the viral envelope with the target membrane. Both approaches provided similar conclusions on the mechanism of MHV-A59 cell entry. MHV-A59 infection was found to be sensitive to substances that interfere with endocytosis and to lysosomotropic agents, pointing to an endocytic uptake and delivery of viruses to an acidic intracellular compartment. The acidic environment triggers the fusion activity of MHV-A59, which is strongly supported by the efficient and fast fusion of the viral envelope with the plasma membrane of 17Cl-1 cells upon lowering the pH. Suppression of fusion potential by preincubation

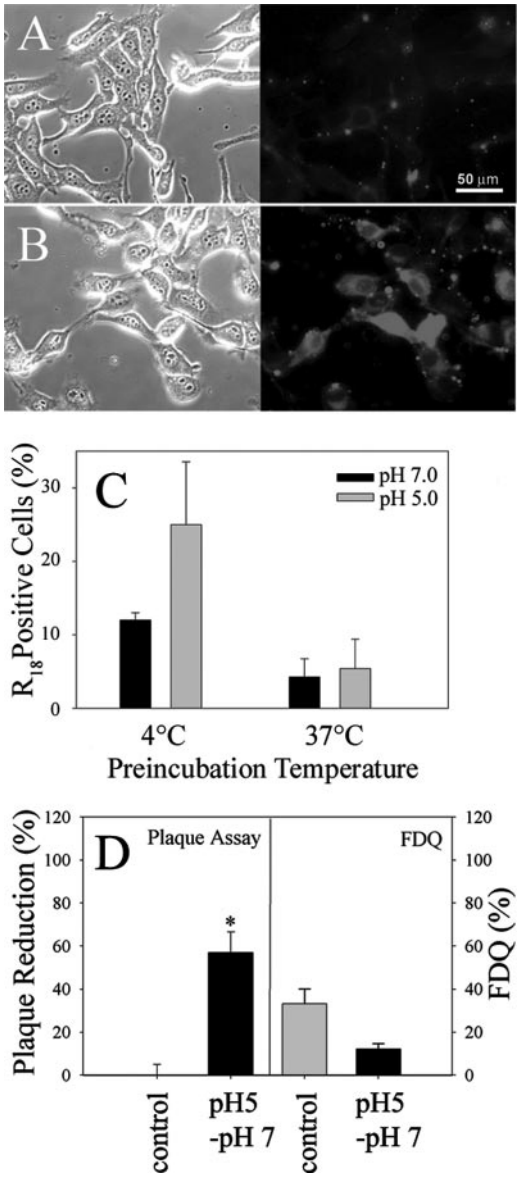

FIG. 7. The fusion activity of MHV-A59 is sensitive to preincubation at low pH. R_{18}-labeled viruses were preincubated at low pH (pH 5.0) for 15 min at either 37°C (A) or 4°C (B) and after neutralization bound to 17Cl-1 cells. Virus-cell complexes were incubated at pH 5.0 and 37°C for 15 min. (A). On the left are differential interference contrast images; on the right are fluorescence images. Bar, 50 μm. (C) Quantification of cells (see panels A and B) showing fusion between R_{18}-labeled viruses and the plasma membrane. Viruses were preincubated as described and subsequently bound to the cells. Virus-cell complexes were incubated at pH 5.0 (black bars) or at pH 7.0 (gray bars) at 37°C for 15 min, and the percentage of R_{18}-positive cells was determined by fluorescence microscopy. (D) Influence of low-pH treatment of MHV-A59 (pH 5.0, 15 min, 37°C) on infectivity (left panel, plaque assay) and fusion activity (right panel, fluorescence dequenching [FDQ]). For the plaque assay, see the legend to Fig. 1. Fusion activity was measured by the fluorescence dequenching assay as shown in Fig. 5. The extent of fluorescence dequenching was measured at $t = 1{,}800$ s (see Fig. 5). The data present the means ± the standard errors of estimates of at least three independent experiments.

of MHV-A59 at acidic pH and electron micrographs of low-pH-treated MHV-A59 suggest that an irreversible conformational change of the S protein triggers fusion between the viral envelope and the target membrane.

All lysosomotropic substances—ammonium chloride, monensin, bafilomycin A1, and concanamycin—suppressed infection of 17Cl-1, LR-7, and DBT cells by MHV-A59. Notably, bafilomycin A1 may interfere with the endocytic route in two different ways. Bafilomycin A1 is known to prevent endosomal acidification by blocking vacuolar proton ATPases, but it also inhibits the transport from early to late endosomes (1, 14). Direct support for the relevance of endocytic uptake for cell entry was provided by the inhibition of MHV-A59 infection with chlorpromazine. It has been shown that chlorpromazine abolishes the formation of clathrin-coated vesicles by interfering with the interaction of the adapter protein AP-2 with the clathrin-coated pit lattice (64) and thus inhibiting clathrin-dependent endocytosis (2, 13, 53, 60). Hence, our results suggest that MHV-A59 enters the cells via the clathrin-mediated pathway. The sensitivity of infection to lysosomotropic agents is consistent with such an entry pathway, since clathrin-coated vesicles deliver their content to endosomes with an acidic environment. This is also in line with a previous report showing a delay in infection cycle for MHV-A59-infected L2 cells treated with ammonium chloride (37). Furthermore, the suppression of infection of cholesterol-depleted cells may support the conclusion that endocytic uptake is the major pathway for cell entry of MHV-A59. It has been shown that clathrin-dependent endocytosis is strongly inhibited after cholesterol depletion by MβCD (49).

The concentrations of various agents interfering either with the endocytic pathway or with the acidification of endosomal compartments have been selected based on previous investigations on endocytic entry and delivery to acidic intracellular organelles of other envelope viruses (for references, see Results). Treatment with these agents did not interfere with cell viability (see Results).

The conclusion that an endocytic compartment plays a key role in the infectious process is in agreement with recent studies of Rottier and coworkers (12). They found that infection of LR-7 cells by MHV-A59 with cleaved spike proteins was sensitive to chlorpromazine and bafilomycin A1. However, the influence of bafilomycin A1 on infection was rather moderate. This could be related to the lower concentration of bafilomycin A1 used in the experimental setup of that study compared to the one used in our study. Indeed, when using concentrations similar to that of 17Cl-1 cells we found the same strong inhibition of MHV-A59 infection of LR-7 and DBT cells by bafilomycin A1. On the contrary, our results are not consistent with those of Weiss and coworkers (48). These authors did not find any suppression of infection of murine fibroblast L2 cells by a recombinant MHV-A59 in either the presence of bafilomycin A1 or ammonium chloride. While in our study, as well as in most of the other studies with either coronaviruses or other enveloped viruses, the lysosomotropic agents were present throughout the whole time course of the experiment, in the experiments of Qui et al. (48) the agents were washed out after 1 h p.i. Thus, we surmise that the recombinant virus MHV-A59 (RA59) remained intact during the incubation time and the recovery of the acidic conditions in the endosomal compart-

ment after removal of the lysosomotropic agents caused activation of the fusion potential.

It has been shown that other coronaviruses such as MHV-2 (48) and SARS-CoV (54) use a pH-dependent entry pathway. However, for these viruses acidification may not directly trigger a conformational change of the S-protein mediating fusion. The pH dependence of infectivity by MHV-2 and SARS viruses relies on proteases as cathepsins (cathepsin L) localized in the late endosome and lysosome that cleave the spike proteins and, in this way, activate their fusion potential. Notably, MHV-2 and SARS-CoV S protein, unlike the spikes encoded by other MHV strains, are not cleaved into S1 and S2 subunits during virus maturation in the host cell. Hence, to gain the fusion activity, the proteins have to be proteolytically cleaved at a later step such as upon cell entry. The activity of endosomal proteases, which may depend on low pH, cleave the viral spike proteins in the endosome, enabling a conformational change that mediates fusion. Indeed, it has been shown that trypsin treatment of the viruses proteolytically activates the fusion activity of the spike proteins (48, 54). Whether the pH may also be important for the conformational change itself is not yet clear. Recently, Li et al. reported a pH-dependent organization of the ectodomain of the SARS-CoV S protein (32).

We found that, in contrast to viruses with uncleaved spike proteins (MHV-A59 FI), MHV-A59 infection did not depend on acidic proteases. The results are in agreement with those of Qiu et al., who showed that MHV-A59 infectivity was only mildly impaired by inhibitors of endosomal proteases (48). This is not surprising since it is known that the S protein becomes cleaved already during maturation of MHV-A59 in 17Cl-1 cells (16). In the presence of protease inhibitors we observed only a moderate decrease of the infection of 17Cl-1 cells by MHV-A59. This might be explained by the possibility that cleavage of the S protein into the S1 and S2 subunits during virus maturation is incomplete and endosomal proteases contribute to the infectivity of MHV-A59. Recently, an increase of infectivity has been observed after trypsin treatment of MHV-A59 maturated from 17Cl-1 cells (16).

Nevertheless, as discussed above, our data suggest that endocytic compartments with an acidic lumen also play a role for entry of MHV-A59 with cleaved spike proteins. Since we could rule out that the activity of intracellular proteases plays a key role, we surmise that the low pH of endocytic compartments triggers fusion directly. Indeed, our fluorescence microscopic data provide clear evidence that acidification is sufficient to trigger fusion of MHV-A59 with the plasma membrane of 17Cl-1 cells. Subsequent to the binding of MHV-A59 to 17Cl-1 cells, we found rapid and efficient fusion with the plasma membrane at 37°C after acidification of the suspension medium, mimicking the luminal pH of the late endosomal compartment. In contrast, merging of the viral envelope with the plasma membrane was not detected at neutral pH. However, after incubation of virus-cell complexes for > 10 min at 37°C, intracellular staining was observed, which could be suppressed by lysosomotropic agents but not in the presence of protease inhibitors. This staining pattern strongly supports that MHV-A59 utilizes the endocytic pathway and is delivered to acidic endosomal compartments, where fusion takes place. We propose that low pH directly triggers a conformational change of the spike proteins activating the fusion potential. This is supported by the observation that preincubation of MHV-A59 at low pH caused an irreversible conformational change of the spike proteins accompanied by the loss of infectivity and fusion activity. The role of acidic pH for infection by MHV-A59 is underscored by the observation that a plaque reduction was also observed when viruses were fused with the plasma membrane of 17Cl-1 cells treated with lysosomotropic agents. Notably, plaque reduction was less efficient compared to cells that were infected via the clathrin-dependent pathway. This may indicate that conditions for productive fusion are suboptimal at the plasma membrane interfering, for example, with the release of the viral genome into the cell and its transport to the nucleus.

The sensitivity of the spike protein ectodomain to low pH has been already reported. A conformational change of the S protein of MHV-A59 has been described at pH 6.5 after binding to its receptor (58, 66, 73). The latter observation may suggest that both interaction with the receptor and low pH play a role in triggering the conformational change of the S protein of MHV. Interaction with the receptor CEACAM has been shown to induce structural alterations of the S protein (35, 73).

The irreversibility of the conformational change and the accompanied loss of the fusion potential are typical for class I fusion proteins independent of whether the structural transition is triggered by receptor interaction (at neutral pH) or by low pH (for a review, see reference 15). A typical example is the fusion mediating hemagglutinin of the influenza virus A, which undergoes a rapid, irreversible conformational change at acidic pH and elevated temperatures (30, 47). However, such an inactivated postfusion conformation was not adopted when low pH incubation of influenza virus was done at low temperature. In that case the fusion capacity was preserved (30, 51). We have made a similar observation for MHV-A59 here. After incubation at pH 5.0 and low temperature, MHV-A59 was still able to fuse with the plasma membrane of 17Cl-1 cells at low pH and elevated temperature. Even at neutral pH we found fusion activity for these virus-cell complexes (see Fig. 7) that were not observed for control virus-cell complexes (no preincubation). This suggests that the S protein is driven to a state committed to fusion by preincubation at acidic pH and low temperature and which is preserved after neutralization. Such a commitment state has been already described for influenza virus A hemagglutinin (30, 51).

We suppose that the irreversible postfusion state of the S protein of MHV-A59 corresponds to a conformation harboring the coiled-coil motif formed by the two heptad repeat sequences HR1 (amino acids 947 to 1082) and HR2 (amino acids 1214 to 1261) as it has been shown for other S proteins of SARS and MHV as well as for other class I fusion proteins (for a review, see reference 15). These two highly conserved sequences form a central three-chain coiled coil by HR1 surrounded by three antiparallel segments of HR2. This so-called six-helix bundle (6HB) is very stable (67, 69–71). The 6HB is considered to play an important role in triggering membrane fusion. Its formation transposes the viral fusion peptide which is inserted into the target membrane and the transmembrane domain of the S2 subunit in close association, thereby enabling a close apposition between the viral envelope and the target membrane (for a review, see reference 15).

Our conclusion that infection by the coronavirus MHV-A59 requires the endocytic delivery of the virus to an acidic compartment and that low pH directly triggers the conformational change of the S protein is in line with recent observations for another member of this virus family, the avian coronavirus infectious bronchitis virus (11). Infection by this virus was abolished by lysosomotropic substances and inhibitors of pH-dependent endocytosis but was not affected by protease inhibitors. Furthermore, pH-dependent fusion could be demonstrated by the fluorescence dequenching assay using R_{18}-labeled virions. In conclusion, this pathway of cell entry and infection is common to various members of the coronavirus family.

ACKNOWLEDGMENTS

We are indebted to J. Ziebuhr for providing the 17Cl-1 cells and the MHV-A59 virus (Ohio 99).

This study was financially supported by grants to A.H. and C.B. from the DFG, Germany.

REFERENCES

1. **Bayer, N., D. Schober, M. Huttinger, D. Blaas, and R. Fuchs.** 2001. Inhibition of clathrin-dependent endocytosis has multiple effects on human rhinovirus serotype 2 cell entry. J. Biol. Chem. **276:**3952–3962.
2. **Blanchard, E., S. Belouzard, L. Goueslain, T. Wakita, J. Dubuisson, C. Wychowski, and Y. Rouille.** 2006. Hepatitis C virus entry depends on clathrin-mediated endocytosis. J. Virol. **80:**6964–6972.
3. **Blumenthal, R., A. Bali-Puri, A. Walter, D. Covell, and O. Eidelman.** 1987. pH-dependent fusion of vesicular stomatitis virus with Vero cells: measurement by dequenching of octadecyl rhodamine fluorescence. J. Biol. Chem. **262:**13614–13619.
4. **Blumenthal, R., S. A. Gallo, M. Viard, Y. Raviv, and A. Puri.** 2002. Fluorescent lipid probes in the study of viral membrane fusion. Chem. Phys. Lipids **116:**39–55.
5. **Bos, E. C., J. C. Dobbe, W. Luytjes, and W. J. Spaan.** 1997. A subgenomic mRNA transcript of the coronavirus mouse hepatitis virus strain A59 defective interfering (DI) RNA is packaged when it contains the DI packaging signal. J. Virol. **71:**5684–5687.
6. **Bosch, B. J., R. van der Zee, C. A. de Haan, and P. J. Rottier.** 2003. The coronavirus spike protein is a class I virus fusion protein: structural and functional characterization of the fusion core complex. J. Virol. **77**:8801–8811.
7. **Chan, D. C., and P. S. Kim.** 1998. HIV entry and its inhibition. Cell **93:**681–684.
8. **Chandran, K., N. J. Sullivan, U. Felbor, S. P. Whelan, and J. M. Cunningham.** 2005. Endosomal proteolysis of the Ebola virus glycoprotein is necessary for infection. Science **308:**1643–1645.
9. **Choi, K. S., H. Aizaki, and M. M. Lai.** 2005. Murine coronavirus requires lipid rafts for virus entry and cell-cell fusion but not for virus release. J. Virol. **79:**9862–9871.
10. **Chu, J. J., and M. L. Ng.** 2004. Infectious entry of West Nile virus occurs through a clathrin-mediated endocytic pathway. J. Virol. **78:**10543–10555.
11. **Chu, V. C., L. J. McElroy, V. Chu, B. E. Bauman, and G. R. Whittaker.** 2006. The avian coronavirus infectious bronchitis virus undergoes direct low-pH-dependent fusion activation during entry into host cells. J. Virol. **80:**3180–3188.
12. **de Haan, C. A., K. Stadler, G. J. Godeke, B. J. Bosch, and P. J. Rottier.** 2004. Cleavage inhibition of the murine coronavirus spike protein by a furin-like enzyme affects cell-cell but not virus-cell fusion. J. Virol. **78:**6048–6054.
13. **Diaz-Griffero, F., A. P. Jackson, and J. Brojatsch.** 2005. Cellular uptake of avian leukosis virus subgroup B is mediated by clathrin. Virology **337:**45–54.
14. **Drose, S., and K. Altendorf.** 1997. Bafilomycins and concanamycins as inhibitors of V-ATPases and P-ATPases. J. Exp. Biol. **200:**1–8.
15. **Earp, L. J., S. E. Delos, H. E. Park, and J. M. White.** 2005. The many mechanisms of viral membrane fusion proteins. Curr. Top. Microbiol. Immunol. **285:**25–66.
16. **Frana, M. F., J. N. Behnke, L. S. Sturman, and K. V. Holmes.** 1985. Proteolytic cleavage of the E2 glycoprotein of murine coronavirus: host-dependent differences in proteolytic cleavage and cell fusion. J. Virol. **56:**912–920.
17. **Gallagher, T. M., C. Escarmis, and M. J. Buchmeier.** 1991. Alteration of the pH dependence of coronavirus-induced cell fusion: effect of mutations in the spike glycoprotein. J. Virol. **65:**1916–1928.
18. **Glomb-Reinmund, S., and M. Kielian.** 1998. The role of low pH and disulfide shuffling in the entry and fusion of Semliki Forest virus and Sindbis virus. Virology **248:**372–381.
19. **Guyader, M., E. Kiyokawa, L. Abrami, P. Turelli, and D. Trono.** 2002. Role for human immunodeficiency virus type 1 membrane cholesterol in viral internalization. J. Virol. **76:**10356–10364.
20. **Helenius, A., M. Marsh, and J. White.** 1982. Inhibition of Semliki Forest virus penetration by lysosomotropic weak bases. J. Gen. Virol. **58**(Pt. 1)**:** 47–61.
21. **Hingley, S. T., I. Leparc-Goffart, S. H. Seo, J. C. Tsai, and S. R. Weiss.** 2002. The virulence of mouse hepatitis virus strain A59 is not dependent on efficient spike protein cleavage and cell-to-cell fusion. J. Neurovirol. **8:**400–410.
22. **Hirano, N., K. Fujiwara, S. Hino, and M. Matumoto.** 1974. Replication and plaque formation of mouse hepatitis virus (MHV-2) in mouse cell line DBT culture. Arch. Gesamte Virusforsch. **44:**298–302.
23. **Hoekstra, D., T. de Boer, K. Klappe, and J. Wilschut.** 1984. Fluorescence method for measuring the kinetics of fusion between biological membranes. Biochemistry **23:**5675–5681.
24. **Hofmann, H., K. Hattermann, A. Marzi, T. Gramberg, M. Geier, M. Krumbiegel, S. Kuate, K. Uberla, M. Niedrig, and S. Pohlmann.** 2004. S protein of severe acute respiratory syndrome-associated coronavirus mediates entry into hepatoma cell lines and is targeted by neutralizing antibodies in infected patients. J. Virol. **78:**6134–6142.
25. **Holmes, K. V., B. D. Zelus, J. H. Schickli, and S. R. Weiss.** 2001. Receptor specificity and receptor-induced conformational changes in mouse hepatitis virus spike glycoprotein. Adv. Exp. Med. Biol. **494:**173–181.
26. **Huang, I. C., B. J. Bosch, F. Li, W. Li, K. H. Lee, S. Ghiran, N. Vasilieva, T. S. Dermody, S. C. Harrison, P. R. Dormitzer, M. Farzan, P. J. Rottier, and H. Choe.** 2006. SARS coronavirus, but not human coronavirus NL63, utilizes cathepsin L to infect ACE2-expressing cells. J. Biol. Chem. **281:**3198–3203.
27. **Huss, M., G. Ingenhorst, S. Konig, M. Gassel, S. Drose, A. Zeeck, K. Altendorf, and H. Wieczorek.** 2002. Concanamycin A, the specific inhibitor of V-ATPases, binds to the V(o) subunit c. J. Biol. Chem. **277:**40544–40548.
28. **Katen, L. J., M. M. Januszeski, W. F. Anderson, K. J. Hasenkrug, and L. H. Evans.** 2001. Infectious entry by amphotropic as well as ecotropic murine leukemia viruses occurs through an endocytic pathway. J. Virol. **75:**5018–5026.
29. **Kooi, C., M. Cervin, and R. Anderson.** 1991. Differentiation of acid-pH-dependent and -nondependent entry pathways for mouse hepatitis virus. Virology **180:**108–119.
30. **Korte, T., K. Ludwig, F. P. Booy, R. Blumenthal, and A. Herrmann.** 1999. Conformational intermediates and fusion activity of influenza virus hemagglutinin. J. Virol. **73:**4567–4574.
31. **Krzystyniak, K., and J. M. Dupuy.** 1984. Entry of mouse hepatitis virus 3 into cells. J. Gen. Virol. **65**((Pt. 1)**:**227–231.
32. **Li, F., M. Berardi, W. Li, M. Farzan, P. R. Dormitzer, and S. C. Harrison.** 2006. Conformational states of the severe acute respiratory syndrome coronavirus spike protein ectodomain. J. Virol. **80:**6794–6800.
33. **Marsh, M., and A. Helenius.** 1989. Virus entry into animal cells. Adv. Virus Res. **36:**107–151.
34. **Matlin, K. S., H. Reggio, A. Helenius, and K. Simons.** 1981. Infectious entry pathway of influenza virus in a canine kidney cell line. J. Cell Biol. **91:**601–613.
35. **Matsuyama, S., and F. Taguchi.** 2002. Receptor-induced conformational changes of murine coronavirus spike protein. J. Virol. **76:**11819–11826.
36. **Miura, H. S., K. Nakagaki, and F. Taguchi.** 2004. N-terminal domain of the murine coronavirus receptor CEACAM1 is responsible for fusogenic activation and conformational changes of the spike protein. J. Virol. **78:**216–223.
37. **Mizzen, L., A. Hilton, S. Cheley, and R. Anderson.** 1985. Attenuation of murine coronavirus infection by ammonium chloride. Virology **142:**378–388.
38. **Mothes, W., A. L. Boerger, S. Narayan, J. M. Cunningham, and J. A. Young.** 2000. Retroviral entry mediated by receptor priming and low pH triggering of an envelope glycoprotein. Cell **103:**679–689.
39. **Nash, T. C., and M. J. Buchmeier.** 1997. Entry of mouse hepatitis virus into cells by endosomal and nonendosomal pathways. Virology **233:**1–8.
40. **Nash, T. C., T. M. Gallagher, and M. J. Buchmeier.** 1995. MHVR-independent cell-cell spread of mouse hepatitis virus infection requires neutral pH fusion. Adv. Exp. Med. Biol. **380:**351–357.
41. **Nawa, M., T. Takasaki, K. Yamada, I. Kurane, and T. Akatsuka.** 2003. Interference in Japanese encephalitis virus infection of Vero cells by a cationic amphiphilic drug, chlorpromazine. J. Gen. Virol. **84:**1737–1741.
42. **Niemann, H., B. Boschek, D. Evans, M. Rosing, T. Tamura, and H. D. Klenk.** 1982. Post-translational glycosylation of coronavirus glycoprotein E1: inhibition by monensin. EMBO J. **1:**1499–1504.
43. **Ohki, S., J. Z. Liu, J. Schaller, and R. C. Welliver.** 2003. The compound DATEM inhibits respiratory syncytial virus fusion activity with epithelial cells. Antivir. Res. **58:**115–124.
44. **Pelkmans, L., and A. Helenius.** 2003. Insider information: what viruses tell us about endocytosis. Curr. Opin. Cell Biol. **15:**414–422.
45. **Perez, L., and L. Carrasco.** 1994. Involvement of the vacuolar H^+-ATPase in animal virus entry. J. Gen. Virol. **75**((Pt. 10)**:**2595–2606.
46. **Popik, W., T. M. Alce, and W. C. Au.** 2002. Human immunodeficiency virus type 1 uses lipid raft-colocalized CD4 and chemokine receptors for productive entry into $CD4^+$ T cells. J. Virol. **76:**4709–4722.
47. **Puri, A., F. P. Booy, R. W. Doms, J. M. White, and R. Blumenthal.** 1990.

Conformational changes and fusion activity of influenza virus hemagglutinin of the H2 and H3 subtypes: effects of acid pretreatment. J. Virol. **64:**3824–3832.
48. **Qiu, Z., S. T. Hingley, G. Simmons, C. Yu, J. Das Sarma, P. Bates, and S. R. Weiss.** 2006. Endosomal proteolysis by cathepsins is necessary for murine coronavirus mouse hepatitis virus type 2 spike-mediated entry. J. Virol. **80:**5768–5776.
49. **Rodal, S. K., G. Skretting, O. Garred, F. Vilhardt, B. van Deurs, and K. Sandvig.** 1999. Extraction of cholesterol with methyl-beta-cyclodextrin perturbs formation of clathrin-coated endocytic vesicles. Mol. Biol. Cell **10**:961–974.
50. **Sanchez-San Martin, C., T. Lopez, C. F. Arias, and S. Lopez.** 2004. Characterization of rotavirus cell entry. J. Virol. **78:**2310–2318.
51. **Schoch, C., R. Blumenthal, and M. J. Clague.** 1992. A long-lived state for influenza virus-erythrocyte complexes committed to fusion at neutral pH. FEBS Lett. **311:**221–225.
52. **Siddell, S., H. Wege, and V. Ter Meulen.** 1983. The biology of coronaviruses. J. Gen. Virol. **64**(Pt. 4)**:**761–776.
53. **Sieczkarski, S. B., and G. R. Whittaker.** 2002. Influenza virus can enter and infect cells in the absence of clathrin-mediated endocytosis. J. Virol. **76:**10455–10464.
54. **Simmons, G., D. N. Gosalia, A. J. Rennekamp, J. D. Reeves, S. L. Diamond, and P. Bates.** 2005. Inhibitors of cathepsin L prevent severe acute respiratory syndrome coronavirus entry. Proc. Natl. Acad. Sci. USA **102:**11876–11881.
55. **Smith, A. E., and A. Helenius.** 2004. How viruses enter animal cells. Science **304:**237–242.
56. **Sodroski, J. G.** 1999. HIV-1 entry inhibitors in the side pocket. Cell **99:**243–246.
57. **Sturman, L. S., K. V. Holmes, and J. Behnke.** 1980. Isolation of coronavirus envelope glycoproteins and interaction with the viral nucleocapsid. J. Virol. **33:**449–462.
58. **Sturman, L. S., C. S. Ricard, and K. V. Holmes.** 1990. Conformational change of the coronavirus peplomer glycoprotein at pH 8.0 and 37°C correlates with virus aggregation and virus-induced cell fusion. J. Virol. **64:**3042–3050.
59. **Sturman, L. S., and K. K. Takemoto.** 1972. Enhanced growth of a murine coronavirus in transformed mouse cells. Infect. Immun. **6:**501–507.
60. **Sun, X., V. K. Yau, B. J. Briggs, and G. R. Whittaker.** 2005. Role of clathrin-mediated endocytosis during vesicular stomatitis virus entry into host cells. Virology **338:**53–60.
61. **Thorp, E. B., and T. M. Gallagher.** 2004. Requirements for CEACAMs and cholesterol during murine coronavirus cell entry. J. Virol. **78:**2682–2692.
62. **Tscherne, D. M., C. T. Jones, M. J. Evans, B. D. Lindenbach, J. A. McKeating, and C. M. Rice.** 2006. Time- and temperature-dependent activation of hepatitis C virus for low-pH-triggered entry. J. Virol. **80:**1734–1741.
63. **van Genderen, I., and G. van Meer.** 1995. Differential targeting of glucosylceramide and galactosylceramide analogues after synthesis but not during transcytosis in Madin-Darby canine kidney cells. J. Cell Biol. **131:**645–654.
64. **Wang, L. H., K. G. Rothberg, and R. G. Anderson.** 1993. Mis-assembly of clathrin lattices on endosomes reveals a regulatory switch for coated pit formation. J. Cell Biol. **123:**1107–1117.
65. **Wege, H., S. Siddell, and V. ter Meulen.** 1982. The biology and pathogenesis of coronaviruses. Curr. Top. Microbiol. Immunol. **99**:165–200.
66. **Weismiller, D. G., L. S. Sturman, M. J. Buchmeier, J. O. Fleming, and K. V. Holmes.** 1990. Monoclonal antibodies to the peplomer glycoprotein of coronavirus mouse hepatitis virus identify two subunits and detect a conformational change in the subunit released under mild alkaline conditions. J. Virol. **64:**3051–3055.
67. **Xu, Y., D. K. Cole, Z. Lou, Y. Liu, L. Qin, X. Li, Z. Bai, F. Yuan, Z. Rao, and G. F. Gao.** 2004. Construct design, biophysical, and biochemical characterization of the fusion core from mouse hepatitis virus (a coronavirus) spike protein. Protein Expr. Purif. **38:**116–122.
68. **Xu, Y., Y. Liu, Z. Lou, L. Qin, X. Li, Z. Bai, H. Pang, P. Tien, G. F. Gao, and Z. Rao.** 2004. Structural basis for coronavirus-mediated membrane fusion: crystal structure of mouse hepatitis virus spike protein fusion core. J. Biol. Chem. **279:**30514–30522.
69. **Xu, Y., Z. Lou, Y. Liu, H. Pang, P. Tien, G. F. Gao, and Z. Rao.** 2004. Crystal structure of severe acute respiratory syndrome coronavirus spike protein fusion core. J. Biol. Chem. **279:**49414–49419.
70. **Xu, Y., N. Su, L. Qin, Z. Bai, G. F. Gao, and Z. Rao.** 2004. Crystallization and preliminary crystallographic analysis of the heptad-repeat complex of SARS coronavirus spike protein. Acta Crystallogr. D Biol. Crystallogr. **60:**2377–2379.
71. **Xu, Y., J. Zhu, Y. Liu, Z. Lou, F. Yuan, D. K. Cole, L. Ni, N. Su, L. Qin, X. Li, Z. Bai, J. I. Bell, H. Pang, P. Tien, G. F. Gao, and Z. Rao.** 2004. Characterization of the heptad repeat regions, HR1 and HR2, and design of a fusion core structure model of the spike protein from severe acute respiratory syndrome (SARS) coronavirus. Biochemistry **43:**14064–14071.
72. **Yonezawa, A., M. Cavrois, and W. C. Greene.** 2005. Studies of ebola virus glycoprotein-mediated entry and fusion by using pseudotyped human immunodeficiency virus type 1 virions: involvement of cytoskeletal proteins and enhancement by tumor necrosis factor alpha. J. Virol. **79:**918–926.
73. **Zelus, B. D., J. H. Schickli, D. M. Blau, S. R. Weiss, and K. V. Holmes.** 2003. Conformational changes in the spike glycoprotein of murine coronavirus are induced at 37°C either by soluble murine CEACAM1 receptors or by pH 8. J. Virol. **77:**830–840.